Inorganic Chemistry

Article

pubs.acs.org/IC

Ba_3LnInS_6 (Ln = Pr, Sm, Gd, Yb) and Ba_2LnGaS_5 (Ln = Pr, Nd): Syntheses, Structures, and Magnetic and Optical Properties

Kai Feng,[†,‡,§] Youguo Shi,[∥] Wenlong Yin,[†,‡,§] Wendong Wang,[⊥] Jiyong Yao,*[,†,‡] and Yicheng Wu[†,‡]

[†]Center for Crystal Research and Development, Technical Institute of Physics and Chemistry, Chinese Academy of Sciences, Beijing 100190, China

[‡]Key Laboratory of Functional Crystals and Laser Technology, Technical Institute of Physics and Chemistry, Chinese Academy of Sciences, Beijing 100190, China

[§]Graduate University of the Chinese Academy of Sciences, Beijing 100049, China

[∥]Beijing National Laboratory for Condensed Matter Physics, Institute of Physics, Chinese Academy of Sciences, Beijing 100190, China

[⊥]School of Science, Beijing University of Post and Telecommunication, Beijing 100876, China

Supporting Information

ABSTRACT: Six new quaternary rare-earth sulfides Ba_3LnInS_6 (Ln = Pr, Sm, Gd, Yb) and Ba_2LnGaS_5 (Ln = Pr, Nd) have been synthesized for the first time. Ba_3LnInS_6 (Ln = Pr, Sm, Gd, Yb) belong to the centrosymmetric space group $R\bar{3}c$ of the trigonal system. The structures contain infinite one-dimensional anionic chains $^{\infty}_{1}[LnInS_6]^{6-}$, which are built from face-sharing LnS_6 distorted triangular prisms and InS_6 octahedra. Ba_2LnGaS_5 (Ln = Pr, Nd) crystallize in the centrosymmetric space group $I4/mcm$ of the tetragonal system. Their structures consist of (BaLn)S layers built from $(BaLn)S_8$ bicapped trigonal prisms. These layers are stacked perpendicular to the c axis and further connected by GaS_4 tetrahedra to form a three-dimensional framework with channels occupied by Ba^{2+} cations. As deduced from magnetic susceptibility measurements on Ba_2NdGaS_5, it is paramagnetic and obeys the Curie–Weiss law. Besides, the band gap of Ba_2NdGaS_5 is determined to be about 2.12(2) eV.

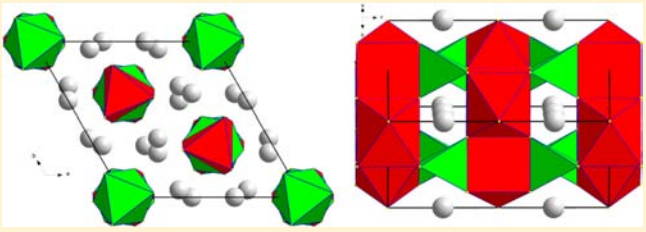

INTRODUCTION

Interest in rare-earth chalcogenides originates not only from their rich structures as a result of the diversity in the geometry of the Ln-centered coordination polyhedra and the connectivity between them but also from the important physical properties related to the 4f electrons.[1,2] In recent years, extensive exploratory synthesis has led to the discovery of many new multinary rare-earth chalcogenides exhibiting interesting structures and physical properties.[3−33] For example, $CsCu_3Dy_2S_5$ and $CsCu_3Er_2S_5$ have an isotypic three-dimensional network $^{\infty}_{3}[Cu_3M_2S_5]^{-}$, spreading along the a axis with large channels, that is well-suited to take up the highly coordinated Cs^+ cations;[34] $KCuCe_2Se_6$ has an interesting structure consisting of two-dimensional $^{\infty}_{2}[CuCe_2Se_6]^{-}$ layers with orderly arranged Cu atoms;[35] in the compounds $BaLn_2FeS_5$ (Ln = Ce, Pr, Nd, Sm), the Fe^{2+} ion exhibits an antiferromagnetic ordering at around 40 K,[36] and $AgPb_mLaTe_{m+2}$ shows high electrical conductivity and a relatively small Seebeck coefficient.[37]

Most of these multinary rare-earth chalcogenides also contain a d-block transition metal. However, increasing attention has recently been paid to chalcogenides containing both f-block rare-earth metals and p-block main-group elements: for example, $K_2Ln_2As_2Se_9$ (Ln = Sm, Gd) contains interesting chairlike As_2Se_4 units,[38] and the $Eu_2Ga_2GeS_7$,[28] La_4InSbS_9,[32] and Sm_4GaSbS_9[27] compounds are found to show strong second-harmonic-generation responses in middle IR. In our research, we think that the quaternary A/Ln/M/Q (A = alkaline-earth metal; Ln = rare earth; M = group IIIA metals Ga and In; Q = S, Se, Te) system is attractive because of the combination of these microscopic nonlinear optical (NLO)-active MQ_4 units with magnetic rare-earth cations in one chalcogenide, and the interplay of the covalent M–Q bonding with the ionic Ln–Q or A–Q bonding may generate compounds with multifunctional properties and interesting structures. Our earlier exploratory efforts have led to the discovery of 12 new selenides in this family, namely, the Ba_2LnMSe_5 (M = Ga, In; Ln = Y, Nd, Sm, Gd, Dy, Er) compounds, which adopt two different structure types for the six Ga-containing selenides and six In-containing selenides, respectively, and exhibit interesting NLO and magnetic properties.[39]

Here, we extend synthetic efforts to the sulfides in this quaternary A/Ln/M/Q (A = alkaline-earth metal; Ln = rare earth; M = group IIIA metals Ga and In; Q = S, Se, Te) system.

Received: August 9, 2012
Published: September 28, 2012

Table 1. Crystal Data and Structure Refinements for Ba_3LnInS_6 (Ln = Pr, Sm, Gd, Yb)[a] and Ba_2LnGaS_5 (Ln = Pr, Nd)[b]

	Ba_3PrInS_6	Ba_3SmInS_6	Ba_3GdInS_6	Ba_3YbInS_6	Ba_2PrGaS_5	Ba_2NdGaS_5
fw	860.11	869.55	876.45	892.24	645.61	648.94
a (Å)	12.1196(2)	12.063(2)	12.072(2)	12.057(2)	8.16340(10)	8.1061(11)
c (Å)	13.9803(5)	13.853(3)	13.816(3)	13.713(3)	13.6093(3)	13.541(3)
V (Å^3)	1778.38(8)	1745.8(5)	1743.6(5)	1726.2(5)	906.94(3)	889.8(2)
ρ_c (g/cm^3)	4.819	4.962	5.008	5.150	4.728	4.844
μ (cm^{-1})	27.95	17.930	18.607	21.158	17.845	18.548
$R(F)^c$	0.0122	0.0199	0.0225	0.0177	0.0204	0.0286
$R_w(F_o^2)^d$	0.0293	0.0383	0.0581	0.0399	0.0467	0.0736

[a]For all four structures, $Z = 6$, space group = $R\bar{3}c$, $T = 153$ (2) K, and $\lambda = 0.71073$ Å. [b]For both structures, $Z = 4$, space group = $I4/mcm$, $T = 153$ (2) K, and $\lambda = 0.71073$ Å. [c]$R(F) = \sum||F_o| - |F_c||/\sum|F_o|$ for $F_o^2 > 2\sigma(F_o^2)$. [d]$R_w(F_o^2) = \{\sum[w(F_o^2 - F_c^2)^2]/\sum wF_o^4\}^{1/2}$ for all data. $w^{-1} = \sigma^2(F_o^2) + (zP)^2$, where $P = (\max(F_o^2, 0) + 2F_c^2)/3$.

To our surprise, the first sulfides that we obtained, with the formula Ba_3LnInS_6 (Ln = Pr, Sm, Gd, Yb), possess stoichiometries and structures different from those of the 12 selenides reported earlier, which clearly demonstrated the richness of the phases in the quaternary A/Ln/M/Q system. The Ba_3LnInS_6 structures feature one-dimensional $^{\infty}_{1}[LnInS_6]^{6-}$ chains of ordered arrays of face-sharing LnS_6 distorted trigonal prisms and InS_6 octahedra. Actually, they represent the first sulfide analogues of the extensively studied hexagonal perovskite-related ($A_3A'BO_6$) oxides, which have displayed very flexible compositions and interesting magnetic and optical properties.[40−42] The investigation into related chalcogenides of the ($A_3A'BO_6$) oxides would be worthwhile because the increased covalence of the metal−chalcogen bond compared to the metal−oxygen bond may have a different influence on the electronic structures and physical properties. Even more interestingly, when we try to replace the In atom of these Ba_3LnInS_6 compounds with a Ga atom, the obtained products are not the hypothetical Ba_3LnGaS_6 compounds but the Ba_2LnGaS_5 (Ln = Pr, Nd) compounds. Although Ba_2LnGaS_5 (Ln = Pr, Nd) possesses the same stoichiometry as the 12 selenides reported earlier, it adopts a structure type totally different from those of the selenides. In this paper, we report the syntheses, structural characterizations, and magnetic and optical properties of Ba_3LnInS_6 (Ln = Pr, Sm, Gd, Yb) and Ba_2LnGaS_5 (Ln = Pr, Nd).

EXPERIMENTAL SECTION

Syntheses. BaS (99%, Sinopharm Chemical Reagent Co., Ltd.), Ga (99.99%, Sinopharm Chemical Reagent Co., Ltd.), In (99.99%, Sinopharm Chemical Reagent Co., Ltd.), S (99.99%, Sinopharm Chemical Reagent Co., Ltd.), and Ln (Ln = Pr, Nd, Sm, Gd, Yb; 99.9%, Alfa Aesar China (Tianjin) Co., Ltd.) were used as received. The binary starting materials Ga_2S_3 and In_2S_3 were prepared from direct reactions of the elements at high temperatures in sealed silica tubes evacuated to 10^{-3} Pa.

Ba_3LnInS_6 (Ln = Pr, Sm, Gd, Yb). The mixtures of BaS (0.339 g, 2 mmol), In_2S_3 (0.163 g, 0.5 mmol), Ln (Ln = Pr, Sm, Gd, Yb; 1 mmol), and S (0.048 g, 1.5 mmol) were ground, loaded into fused-silica tubes under an argon atmosphere in a glovebox, then flame-sealed under a high vacuum of 10^{-3} Pa. The tubes were then placed in computer-controlled furnaces, heated to 1323 K in 24 h, left for 48 h, cooled to 693 K at a rate of 3 K/h, and finally cooled to room temperature by switching off the furnace. Dark-red crystals were found in the ampules. The crystals were stable in air.

The chip-shaped crystals were manually selected for structure characterization and determined as Ba_3LnInS_6 (Ln = Pr, Sm, Gd, Yb). Analyses of the crystals with an energy-dispersive X-ray (EDX)-equipped Hitachi S-4800 scanning electron microscope showed the presence of Ba, Ln, In, and S in the approximate ratio of 3:1:1:6.

Ba_2LnGaS_5 (Ln = Pr, Nd). The mixtures of BaS (0.339 g, 2 mmol), Ga_2S_3 (0.118 g, 0.5 mmol), Ln (Ln = Pr, Nd; 1 mmol), and S (0.048 g, 1.5 mmol) were ground, loaded into fused-silica tubes under an argon atmosphere in a glovebox, and then flame-sealed under a high vacuum of 10^{-3} Pa. The tubes were then placed in computer-controlled furnaces, heated to 1323 K in 24 h, left for 48 h, cooled to 693 K at a rate of 3 K/h, and finally cooled to room temperature by switching off the furnace. Dark-red crystals were found in the ampules. The crystals were stable in air.

The chip-shaped crystals were manually selected for structure characterization and determined as Ba_2LnGaS_5 (Ln = Pr, Nd). Analyses of the crystals with an EDX-equipped Hitachi S-4800 scanning electron microscope showed the presence of Ba, Ga, Ln, and S in the approximate ratio of 2:1:1:5. Inductively coupled plasma (ICP) measurement on the crystals indicated that the molar ratio of Ba/Ln/Ga is close to 2:1:1.

Structure Determination. The single-crystal X-ray diffraction measurements were performed on a Rigaku AFC10 diffractometer quipped with graphite-monochromated K_α ($\lambda = 0.71073$ Å) radiation at 153 K. The *CrystalClear* software[43] was used for data extraction and integration, and the program *XPREP*[44] was used for face-indexed absorption corrections.

The structure was solved with direct methods implemented in the program *SHELXS* and refined with the least-squares program *SHELXL* of the *SHELXTL.PC* suite of programs.[44] For Ba_3LnInS_6 (Ln = Pr, Sm, Gd, Yb), one Ba position (Wyckoff site 18e), one Ln position (Wyckoff site 6a), one In position (Wyckoff site 6b), and one S position (Wyckoff site 36f) were found. It was straightforward to refine the structure of the compounds containing the larger rare-earth cations, namely, Pr^{3+}, Sm^{3+}, and Gd^{3+}: the anisotropic displacement parameters of all atoms are normal, and refinement of the occupancy of all atoms led to values very close to 100% occupancy, which indicated no detectable disorder between the Ln^{3+} and In^{3+} cations in these compounds. However, in the initial structure refinement of Ba_3YbInS_6, which contains the smaller rare-earth element Yb, the isotropic displacement parameter of Yb was unusually large, while that of In was close to zero, which was indicative of possible disorder between the Yb and In cations. Subsequently, disorder of Yb and In was introduced at Yb (Wyckoff site 6a) and In (Wyckoff site 6b) positions, and the refinements showed that Yb and In were disordered at the Yb (Wyckoff site 6a) and In (Wyckoff site 6b) positions with Yb/In ratios of 0.840:0.160 and 0.158:0.842, respectively. The resultant R index R1/wR2 decreased from 0.0261/0.0885 to 0.0177/0.0399 and the largest peak/hole in the difference electron density map was reduced from 4.57/−2.82 to 0.88/−1.16 e/Å^3 with this disorder model. Considering that virtually the same total amounts of Yb and In cations in the structure were present, the final stoichiometry was also determined as Ba_3YbInS_6.

For Ba_2LnGaS_5 (Ln = Pr, Nd), three metal positions are found: M1 (Wyckoff site 4a) surrounded by about 10 S atoms with a M1−S distance of about 3.4 Å, M2 (Wyckoff site 8h) coordinated to 8 S atoms at a distance of around 3.0 Å, and M3 (Wyckoff site 4b) coordinated to 4 S atoms at a distance of around 2.2 Å. In addition,

dx.doi.org/10.1021/ic301750x | Inorg. Chem. 2012, 51, 11144−11149

two S atoms (Wyckoff sites 4c and 16l) were decided. On the basis of the bond lengths and the electron density, Ba can be assigned to the M1 position and Ga to the M3 position, respectively. From the bond length, the Ln atom should take the M2 position. However, if the M2 position is totally occupied by the Ln elements, the resultant composition $BaLn_2GaS_5$ neither agrees with the EDX or ICP results regarding the elemental ratios in these compounds nor satisfies the charge-balance requirements. A disordered model was then tried, in which the M2 position was occupied by both Ba and Ln atoms. The resultant occupancy of Ba at the M2 position is close to 50%. Hence, the M2 position is set to be occupied by Ba and Ln in a ratio of 1:1 in the final refinement, leading to the formula of Ba_2LnGaS_5 (Ln = Pr, Nd), which agrees with the elemental analysis results by EDX and ICP and achieves charge balance. Similar structural features were found in the Sr_2EuAlO_5 and Sr_2EuFeO_5 oxides.[45]

The final refinements of all structures include anisotropic displacement parameters and secondary extinction correction. The program *STRUCTURE TIDY*[46] was then employed to standardize the atomic coordinates. Additional experimental details are given in Table 1, and selected metrical data are given in Tables 2 and 3. Further information may be found in the Supporting Information.

Table 2. Selected Interatomic Distances (Å) for Ba_3LnInS_6 (Ln = Pr, Sm, Gd, Yb)

	Ba_3PrInS_6	Ba_3SmInS_6	Ba_3GdInS_6	Ba_3YbInS_6
Ba−S×2	3.171(1)	3.151(1)	3.154(2)	3.147(1)
Ba−S×2	3.233(1)	3.225(1)	3.232(1)	3.251(1)
Ba−S×2	3.300(1)	3.286(1)	3.288(2)	3.287(1)
Ba−S×2	3.335(1)	3.316(1)	3.318(1)	3.311(1)
Ln−S×6	2.836(1)	2.799(1)	2.784(1)	2.735(1)
In−S×6	2.633(1)	2.624(1)	2.622(2)	2.620(1)

Table 3. Selected Interatomic Distances (Å) for Ba_2LnGaS_5 (Ln = Pr, Nd)

	Ba_2PrGaS_5	Ba_2NdGaS_5
Ba1−S1×2	3.402(1)	3.385(1)
Ba1−S2×8	3.442(1)	3.421(2)
Ln−S2×2	2.922(1)	2.901(2)
Ln−S1×2	3.056(1)	3.036(1)
Ln−S2×4	3.200(1)	3.174(2)
Ga−S2×4	2.246(1)	2.239(2)

Magnetic Susceptibility Measurements. Because of the low yields in our synthesis and the tiny size of the obtained crystals, only enough Ba_2NdGaS_5 crystals can be picked for measuring the magnetic susceptibility. A SQUID magnetometer (Quantum Design) operating at 10 kOe was used to carry out magnetic susceptibility measurements on Ba_2NdGaS_5. The zero-field-cooled and field-cooled (ZFC/FC) magnetic susceptibility was obtained in the temperature range of 2−300 K on ground crystals in a gelatin capsule.

Diffuse-Reflectance Spectroscopy. A Cary 5000 UV−visible−near-IR (NIR) spectrophotometer with a diffuse-reflectance accessory was used to measure the spectrum of Ba_2NdGaS_5 over the range 400 nm (3.10 eV) to 1300 nm (0.95 eV).

RESULTS AND DISCUSSION

Synthesis. Six sulfides Ba_3LnInS_6 (Ln = Pr, Sm, Gd, Yb) and Ba_2LnGaS_5 (Ln = Pr, Nd) have been synthesized by traditional high-temperature solid-state reactions for the first time. The yields range from 10% to 20% based on Ln. Great efforts have been made to synthesize analogues containing other rare-earth elements available to us, namely, Y, La, Ce, Nd, Dy, Er, and Lu for Ba_3LnInS_6 and Y, La, Ce, Sm, Gd, Dy, Er, Yb, and Lu for Ba_2LnGaS_5, but it did not work. Thus, we only report here the six members that we obtained.

Structure of Ba_3LnInS_6 (Ln = Pr, Sm, Gd, Yb). The four compounds Ba_3LnInS_6 (Ln = Pr, Sm, Gd, Yb) are isotypic and crystallize in the K_4CdCl_6 structure type,[47] which is in the centrosymmetric trigonal space group $R\bar{3}c$. The asymmetric unit of Ba_3LnInS_6 (Ln = Pr, Sm, Gd, Yb) contains one crystallographically independent Ba atom, one Ln atom, one In atom, and one S atom, which are at Wyckoff positions 18e, 6a, 6b, and 36f, respectively. Without metal−metal or S−S bonds in the structures, the oxidation states of 2+, 3+, 3+, and 2− can be assigned to Ba, In, Ln, and S, respectively.

The structure of Ba_3GdInS_6 is illustrated in Figure 1. The basic structural unit of Ba_3GdInS_6 is an infinite one-dimensional

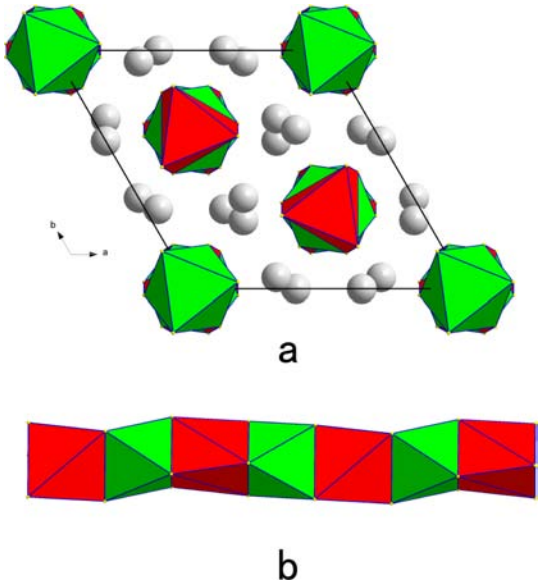

Figure 1. Crystal structure (a) and the $^{\infty}_{1}[GdInS_6]^{6-}$ anionic chain (b) of Ba_3GdInS_6 (GdS_6 and InS_6 polyhedra are shaded in red and green, respectively; the white balls are Ba atoms).

$^{\infty}_{1}[GdInS_6]^{6-}$ anionic chain built from InS_6 octahedra (oct) and GdS_6 distorted triangular prisms (tp), which are connected alternately via face-sharing to form chains along the *c*-axis direction, which are separated by Ba atoms in a bicapped trigonal-prismatic geometry. The compound Ba_4CrUS_9[48] possesses a similar structure with one-dimensional $^{\infty}_{1}[Cr_2US_9]^{8-}$ chains separated by Ba^{2+} cations. $^{\infty}_{1}[Cr_2US_9]^{8-}$ is a chain built from CrS_6 octahedra and US_6 trigonal prisms in the sequence *oct oct tp oct oct tp*, while for $^{\infty}_{1}[GdInS_6]^{6-}$, InS_6 octahedra and GdS_6 distorted triangular prisms arrange in the sequence of *oct tp oct tp*. In addition, there are two crystallographically unique one-dimensional chains in Ba_4CrUS_9, but only one exists in Ba_3GdInS_6.

The selected bond distances of Ba_3LnInS_6 (Ln = Pr, Sm, Gd, Yb) are listed in Table 2. The Ba−S distances of 3.171(1)−3.335(1) Å are similar to those of Ba_2AgInS_4 [3.128(2)−3.314(2) Å] for eight-coordinated Ba;[49] The In−S distances lie in the range of 2.620(1)−2.633(1) Å, close to those of $Bi_3In_4S_{10}$ [2.51(1)−2.82(2) Å] for six-coordinated In atoms.[50] The Ln−S distances are also normal for the six-coordinated Ln cations: the Pr−S distance of 2.836(1) Å is comparable to those in $BaPr_2MnS_5$ [2.773(7)−3.081(7) Å],[51] the Sm−S distance of 2.799(1) Å is similar to those in $BaSm_2FeS_5$ [2.752(1)−

dx.doi.org/10.1021/ic301750x | *Inorg. Chem.* 2012, 51, 11144−11149

3.017(1) Å],[52] the Gd−S distance of 2.784(1) Å resembles those in $Ba_4Gd_2Cd_3S_{10}$ [2.765(3)−2.799(3) Å],[53] and the Yb−S distance of 2.735(1) Å agrees with those in $CaYbInS_4$ [2.678(1)−2.694(2) Å].[3] In addition, it is interesting to note that twist angles between the pair of triangular faces (15.604°, 15.745°, 15.817°, and 15.987° for Ln = Pr, Sm, Gd, and Yb, respectively) increase with a decrease of the Ln^{3+} ion radius.

Structure of Ba_2LnGaS_5 (Ln = Pr, Nd). The two compounds Ba_2LnGaS_5 (Ln = Pr, Nd) are isostructural and crystallize in the Cs_3CoCl_5 structure type of centrosymmetric tetragonal space group $I4/mcm$.[54] In the asymmetric unit of Ba_2LnGaS_5 (Ln = Pr, Nd), Ba1, Ga, S1 and S2 atoms are at Wyckoff positions 4a, 4b, 4c, and 16l with 100% occupancy, respectively, while the Ba2 and Ln atoms are disordered at Wyckoff position 8h with 50% occupancy for each atom. Because there are no metal−metal or S−S bonds in the structures, the oxidation states of 2+, 3+, 3+, and 2− can be assigned to Ba, Ga, Ln, and S, respectively.

The structure of Ba_2NdGaS_5 is shown in Figure 2. Each Ga atom is coordinated to four S atoms to form perfect GaS_4 tetrahedra with four identical Ga−S bonds. The Nd(Ba2) atom is joined to eight S atoms to form a bicapped trigonal prism (btp). Ba1 atoms are coordinated by 10 S atoms. As shown in Figure 2, one $Nd(Ba2)S_8$ bicapped trigonal prism (btp) is linked to one nearest-adjacent $Nd(Ba2)S_8$ btp by sharing the four-membered face and to four next-nearest-neighboring $Nd(Ba2)S_8$ btp's by sharing the three-membered faces, and in this way, a two-dimensional anionic (BaNd)S layer was generated. The layers are stacked along the c axis and further connected by isolated GaS_4 tetrahedra to form a three-dimensional framework with channels occupied by Ba atoms along the [110] direction. The structure of Ba_2GaNdS_5 is similar to that of $BaLn_2FeS_5$,[53] except that the Wyckoff 8h metal position was occupied by Ln metals only in the $BaLn_2FeS_5$ series of compounds. Another isostructural series of compounds are the Sr_2EuAlO_5 and Sr_2EuFeO_5 oxides,[45] in which the Wyckoff 8h metal position was half-occupied by Eu atoms and half-occupied by Sr atoms, just as in the case of Ba_2LnGaS_5 (Ln = Pr, Nd).

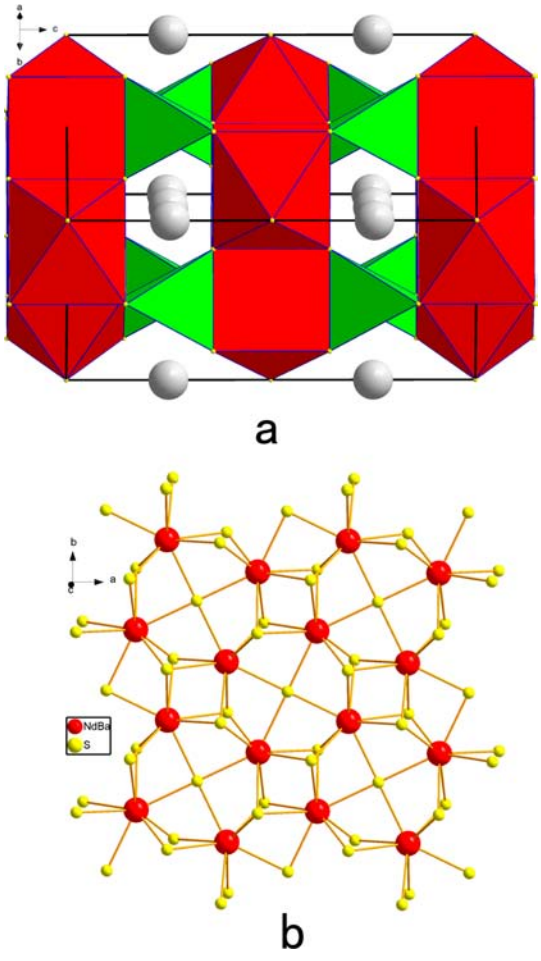

Figure 2. Crystal structure seen along the [110] direction (a) and the Nd(Ba2)S layer (b) of Ba_2NdGaS_5 [$Nd(Ba2)S_8$ and GaS_4 polyhedra are shaded in red and green, respectively; the white balls are Ba atoms].

In comparison, the corresponding selenides $Ba_2LnGaSe_5$ (Ln = Y, Nd, Sm, Gd, Dy, Er) crystallize in the space group $P\bar{1}$ of the triclinic system, and the structure features a one-dimensional $^{\infty}_{1}[LnGaSe_5]^{4-}$ chain built from $LnSe_6$ octahedra and $GaSe_4$ tetrahedra and separated by Ba^{2+} cations. Because of the smaller size of the S atoms, Ln atoms can be coordinated by two more S atoms in the sulfides than in the selenides. The more surrounding S atoms, in turn, will enhance the opportunity of connecting among these LnS_8 polyhedra, leading to a denser framework, such as that in Ba_2LnGaS_5 (Ln = Pr, Nd).

The selected bond distances of Ba_2LnGaS_5 (Ln = Pr, Nd) are listed in Table 3. The distances of the Ga−S bonds are 2.239(2) Å for Ba_2NdGaS_5 and 2.246(1) Å for Ba_2PrGaS_5, which agree with those of 2.212(1)−2.239(1) Å in $BaGa_2SiS_6$ for tetrahedrally coordinated Ga atoms.[54] The Ba−S distances of 3.385(1)−3.442(1) Å are similar to those of $BaGa_2SiS_6$ [3.474(1)−3.6320(8) Å].[54] The Pr−S [2.922(1)−3.200(1) Å] and Nd−S [2.901(2)−3.174(2) Å] distances are a little larger than the 2.773(7)−3.081(7) Å distances of Pr−S in $BaPr_2MnS_5$[52] and the 2.754(8)−3.079(8) Å distances of Nd−S in $BaNd_2MnS_5$.[55] Such a deviation may result from the occupation of Ba in these Ln positions because the Ba^{2+} cation has a larger radius than the Ln^{3+} cation.

Magnetic Susceptibility Measurement. Figure 3 shows the temperature variation of the molar magnetic susceptibility (χ_m) and the inverse magnetic susceptibility ($1/\chi_m$) for the Ba_2NdGaS_5 compound. The ZFC and FC magnetic susceptibility data are essentially superimposable at all temperatures.

The magnetic susceptibility data of the Ba_2NdGaS_5 sample were fitted by a least-squares method to a modified Curie−

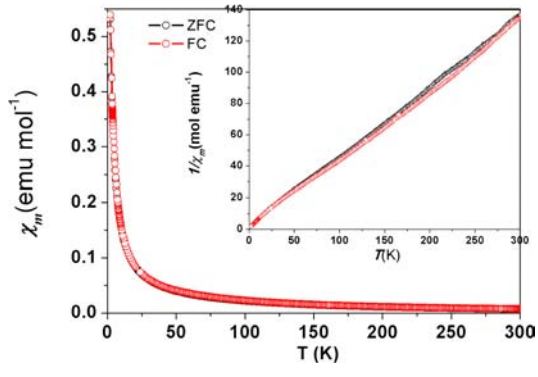

Figure 3. χ_m versus temperature of Ba_2NdGaS_5 for FC and ZFC data. Inset: plot of $1/\chi_m$ versus temperature.

dx.doi.org/10.1021/ic301750x | Inorg. Chem. 2012, 51, 11144−11149

Weiss law: $\chi_m = C/(T - \theta)$, where C is the Curie constant and θ is the Weiss constant. The effective magnetic moment [μ_{eff}(total)] was calculated from the equation μ_{eff}(total) = $(7.997C)^{1/2}\mu_B$.[56]

As shown, it is paramagnetic and obeys the Curie–Weiss law over the entire experimental temperature range. As deduced from the fitting results, the values of C and θ for Ba_2NdGaS_5 are 2.25 and 3.69, respectively. The calculated effective magnetic moment is 4.24 μ_B/Nd atom, which is a little bigger than the calculated theoretical value for the Nd^{3+} ion (3.62 μ_B/Nd atom).[57] The divergence between ZFC and FC data within the 200–250 K range may be from a tiny amount of an impure phase, which is attached on the surfaces of the picked crystals and is impossible to get rid of.

Experimental Band Gap. On the basis of the UV–visible–NIR diffuse-reflectance spectra of Ba_2NdGaS_5 (Figure 4), the band gap can be deduced by a straightforward extrapolation method.[58] The absorption edge of Ba_2NdGaS_5 is about 585 nm (2.12 eV) and agrees with the dark-red color. As can be seen, the existence of typical f–f transitions of Nd^{3+} ions brings several broad absorption bands below the optical band gaps between 500 and 950 nm.[22]

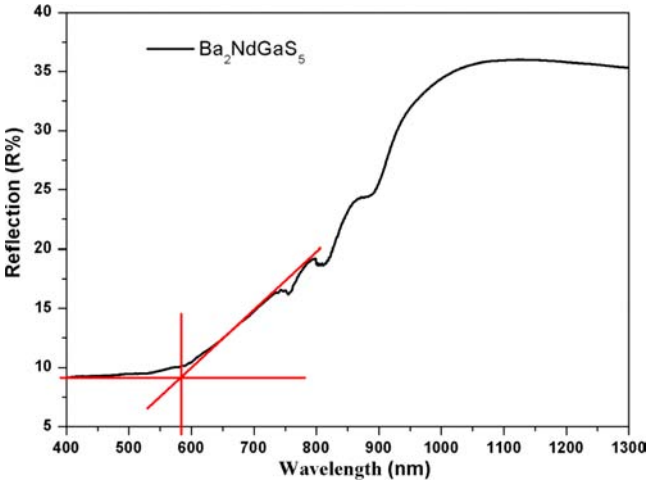

Figure 4. Diffuse-reflectance spectra of Ba_2NdGaS_5.

CONCLUSIONS

In summary, six new rare-earth sulfides in the quaternary A/Ln/M/Q (A = alkaline earth; Ln = rare earth; M = group IIIA metals Ga and In; Q = S, Se, Te) system, Ba_3LnInS_6 (Ln = Pr, Sm, Gd, Yb) and Ba_2LnGaS_5 (Ln = Pr, Nd), have been discovered and characterized. Ba_3LnInS_6 (Ln = Pr, Sm, Gd, Yb) crystallizes in the centrosymmetric space group $R\bar{3}c$ of the trigonal system with infinite one-dimensional anionic chains $^{\infty}_{1}[LnInS_6]^{6-}$ consisting of alternating LnS_6 distorted triangular prisms and InS_6 octahedra in the sequence of *oct tp oct tp*. Ba_2LnGaS_5 (Ln = Pr, Nd) crystallizes in the centrosymmetric space group $I4/mcm$. They possess a three-dimensional framework structure built from $(Ba/Nd)S_8$ bicapped trigonal prisms and GaS_4 tetrahedra. The Ba atoms reside in the channels in the framework. Ba_2NdGaS_5 exhibits paramagnetic behavior, obeying the Curie–Weiss law down to 2 K. In addition, the band gap of Ba_2NdGaS_5 is 2.12(2) eV according to the diffuse-reflectance measurement. These compounds may have potential use as magnetic semiconductors or optical filters.

ASSOCIATED CONTENT

Supporting Information

Crystallographic file in CIF format for Ba_3LnInS_6 (Ln = Pr, Sm, Gd, Yb) and Ba_2LnGaS_5 (Ln = Pr, Nd). This material is available free of charge via the Internet at http://pubs.acs.org.

AUTHOR INFORMATION

Corresponding Author

*E-mail: jyao@mail.ipc.ac.cn.

Notes

The authors declare no competing financial interest.

ACKNOWLEDGMENTS

This research was supported by the National Basic Research Project of China (Grant 2010CB630701), National Natural Science Foundation of China (Grant 91122034), and the Ministry of Science and Technology of China (973 Project 2011CBA00110).

REFERENCES

(1) Flahaut, J. *Handbook on the Physics and Chemistry of Rare Earths*; Elsevier: New York, 1979; Vol. 4, pp 1–88.
(2) Cotton, S. *Lanthanide and Actinides*; Oxford University Press: New York, 1991.
(3) Carpenter, J. D.; Hwu, S. J. *Chem. Mater.* **1992**, *4*, 1368–1372.
(4) Bucher, C. K.; Hwu, S. J. *Inorg. Chem.* **1994**, *33*, 5831–5835.
(5) Sutorik, A. C.; Albrittonthomas, J.; Kannewurf, C. R.; Kanatzidis, M. G. *J. Am. Chem. Soc.* **1994**, *116*, 7706–7713.
(6) Carpenter, J. D.; Hwu, S. J. *Inorg. Chem.* **1995**, *34*, 4647–4651.
(7) Sutorik, A. C.; Albrittonthomas, J.; Hogan, T.; Kannewurf, C. R.; Kanatzidis, M. G. *Chem. Mater.* **1996**, *8*, 751–761.
(8) Patschke, R.; Brazis, P.; Kannewurf, C. R.; Kanatzidis, M. *Inorg. Chem.* **1998**, *37*, 6562–6563.
(9) Patschke, R.; Heising, J.; Kanatzidis, M.; Brazis, P.; Kannewurf, C. R. *Chem. Mater.* **1998**, *10*, 695.
(10) Huang, F. Q.; Ibers, J. A. *Inorg. Chem.* **1999**, *38*, 5978–5983.
(11) Aitken, J. A.; Larson, P.; Mahanti, S. D.; Kanatzidis, M. G. *Chem. Mater.* **2001**, *13*, 4714–4721.
(12) Evenson, C. R.; Dorhout, P. K. *Inorg. Chem.* **2001**, *40*, 2409–2414.
(13) Huang, F. Q.; Mitchell, K.; Ibers, J. A. *Inorg. Chem.* **2001**, *40*, 5123–5126.
(14) Mitchell, K.; Haynes, C. L.; McFarland, A. D.; Van Duyne, R. P.; Ibers, J. A. *Inorg. Chem.* **2002**, *41*, 1199–1204.
(15) Mitchell, K.; Ibers, J. A. *Chem. Rev.* **2002**, *102*, 1929–1952.
(16) Mitchell, K.; Huang, F. Q.; McFarland, A. D.; Haynes, C. L.; Somers, R. C.; Van Duyne, R. P.; Ibers, J. A. *Inorg. Chem.* **2003**, *42*, 4109–4116.
(17) Mitchell, K.; Huang, F. Q.; Caspi, E. N.; McFarland, A. D.; Haynes, C. L.; Somers, R. C.; Jorgensen, J. D.; Van Duyne, R. P.; Ibers, J. A. *Inorg. Chem.* **2004**, *43*, 1082–1089.
(18) Wakeshima, M.; Furuuchi, F.; Hinatsu, Y. *J. Phys.: Condens. Matter* **2004**, *16*, 5503–5518.
(19) Yao, J. Y.; Deng, B.; Sherry, L. J.; McFarland, A. D.; Ellis, D. E.; Van Duyne, R. P.; Ibers, J. A. *Inorg. Chem.* **2004**, *43*, 7735–7740.
(20) Zeng, H.-Y.; Mattausch, H.; Simon, A.; Zheng, F.-K.; Dong, Z.-C.; Guo, G.-C.; Huang, J.-S. *Inorg. Chem.* **2006**, *45*, 7943–7946.
(21) Chan, G. H.; Sherry, L. J.; Van Duyne, R. P.; Ibers, J. A. *Z. Anorg. Allg. Chem.* **2007**, *633*, 1343–1348.
(22) Choudhury, A.; Dorhout, P. K. *Inorg. Chem.* **2008**, *47*, 3603–3609.
(23) Liu, Y.; Chen, L.; Wu, L.-M. *Inorg. Chem.* **2008**, *47*, 855–862.
(24) Guo, S.-P.; Guo, G.-C.; Wang, M.-S.; Zou, J.-P.; Xu, G.; Wang, G.-J.; Long, X.-F.; Huang, J.-S. *Inorg. Chem.* **2009**, *48*, 7059–7065.
(25) Zhao, H.-J.; Li, L.-H.; Wu, L.-M.; Chen, L. *Inorg. Chem.* **2009**, *48*, 11518–11524.

(26) Zhao, H.-J.; Li, L.-H.; Wu, L.-M.; Chen, L. *Inorg. Chem.* **2010**, *49*, 5811−5817.
(27) Chen, M.-C.; Li, L.-H.; Chen, Y.-B.; Chen, L. *J. Am. Chem. Soc.* **2011**, *133*, 4617−4624.
(28) Chen, M.-C.; Li, P.; Zhou, L.-J.; Li, L.-H.; Chen, L. *Inorg. Chem.* **2011**, *50*, 12402−12404.
(29) Jin, G. B.; Choi, E. S.; Guertin, R. P.; Booth, C. H.; Albrecht-Schmitt, T. E. *Chem. Mater.* **2011**, *23*, 1306−1314.
(30) Meng, C.-Y.; Chen, H.; Wang, P.; Chen, L. *Chem. Mater.* **2011**, *23*, 4910−4919.
(31) Bera, T. K.; Kanatzidis, M. G. *Inorg. Chem.* **2012**, *51*, 4293−4299.
(32) Zhao, H.-J.; Zhang, Y.-F.; Chen, L. *J. Am. Chem. Soc.* **2012**, *134*, 1993−1995.
(33) Chan, G. H.; Lee, C.; Dai, D.; Whangbo, M.-H.; Ibers, J. A. *Inorg. Chem.* **2008**, *47*, 1687−1692.
(34) Lauxmann, P.; Schleid, T. *Z. Naturforsch. B* **2001**, *56*, 1149−1154.
(35) Klawitter, Y.; Nather, C.; Jess, I.; Bensch, W.; Kanatzidis, M. G. *Solid State Sci.* **1999**, *1*, 421−431.
(36) Wakeshima, M.; Ino, K.; Hinatsu, Y.; Ishii, Y. *Bull. Chem. Soc. Jpn.* **2003**, *76*, 1519−1525.
(37) Ahn, K.; Li, C.-P.; Uher, C.; Kanatzidis, M. G. *Chem. Mater.* **2009**, *22*, 876−882.
(38) Wu, Y.; Bensch, W. *Inorg. Chem.* **2009**, *48*, 2729−2731.
(39) Yin, W.; Feng, K.; Wang, W.; Shi, Y.; Hao, W.; Yao, J.; Wu, Y. *Inorg. Chem.* **2012**, *51*, 6860−6867.
(40) Layland, R. C.; Kirkland, S. L.; Nunez, P.; zur Loye, H. C. *J. Solid State Chem.* **1998**, *139*, 416−421.
(41) Layland, R. C.; Kirkland, S. L.; zur Loye, H. C. *J. Solid State Chem.* **1998**, *139*, 79−84.
(42) Davis, M. J.; Smith, M. D.; zur Loye, H. C. *J. Solid State Chem.* **2003**, *173*, 122−129.
(43) *CrystalClear*; Rigaku Corp.: Tokyo, 2008.
(44) Sheldrick, G. M. *Acta Crystallogr., Sect. A: Found. Crystallogr.* **2008**, *64*, 112−122.
(45) Drofenik, M.; Golic, L. *Acta Crystallogr., Sect. B: Struct. Sci.* **1979**, *35*, 1059−1062.
(46) Gelato, L. M.; Parthe, E. *J. Appl. Crystallogr.* **1987**, *20*, 139−143.
(47) Beck, H. P.; Milius, W. *Z. Anorg. Allg. Chem.* **1986**, *539*, 7−17.
(48) Yao, J.; Ibers, J. A. *Z. Anorg. Allg. Chem.* **2008**, *634*, 1645−1647.
(49) Yin, W.; Feng, K.; Mei, D.; Yao, J.; Fu, P.; Wu, Y. *Dalton Trans.* **2012**, *41*, 2272−2276.
(50) Yin, W.; Mei, D.; Yao, J.; Fu, P.; Wu, Y. *J. Solid State Chem.* **2010**, *183*, 2544−2551.
(51) Wakeshima, M.; Hinatsu, Y. *J. Solid State Chem.* **2000**, *153*, 330−335.
(52) Ino, K.; Wakeshima, M.; Hinatsu, Y. *Mater. Res. Bull.* **2001**, *36*, 2207−2213.
(53) Yang, Y. T.; Ibers, J. A. *J. Solid State Chem.* **2000**, *149*, 384−390.
(54) Powell, H. M.; Wells, A. F. *J. Chem. Soc.* **1935**, 359−362.
(55) Yin, W.; Feng, K.; He, R.; Mei, D.; Lin, Z.; Yao, J.; Wu, Y. *Dalton Trans.* **2012**, *41*, 5653−5661.
(56) O'Connor, C. J. Magnetochemistry—Advances in Theory and Experimentation. *Progress in Inorganic Chemistry*; John Wiley & Sons, Inc.: New York, 2007; pp 203−283.
(57) Van Vleck, J. H. *The Theory of Electric and Magnetic Susceptibilities*; Oxford University Press: Oxford, U.K., 1932; pp 226−261.
(58) Schevciw, O.; White, W. B. *Mater. Res. Bull.* **1983**, *18*, 1059−1068.